Prospects for producing ultracold NH_3 molecules by sympathetic cooling: A survey of interaction potentials

Piotr S. Żuchowski* and Jeremy M. Hutson†
Department of Chemistry, Durham University, South Road, DH1 3LE, United Kingdom
(Received 13 May 2008; published 1 August 2008)

We investigate the possibility of producing ultracold NH_3 molecules by sympathetic cooling in a bath of ultracold atoms. We consider the interactions of NH_3 with alkali-metal and alkaline-earth-metal atoms, and with Xe, using *ab initio* coupled-cluster calculations. For Rb-NH_3 and Xe-NH_3 we develop full potential energy surfaces, while for the other systems we characterize the stationary points (global and local minima and saddle points). We also calculate isotropic and anisotropic van der Waals C_6 coefficients for all the systems. The potential energy surfaces for interaction of NH_3 with alkali-metal and alkaline-earth-metal atoms all show deep potential wells and strong anisotropies. The well depths vary from 887 cm^{-1} for Mg-NH_3 to 5104 cm^{-1} for Li-NH_3. This suggests that all these systems will exhibit strong inelasticity whenever inelastic collisions are energetically allowed and that sympathetic cooling will work only when both the atoms and the molecules are already in their lowest internal states. Xe-NH_3 is more weakly bound and less anisotropic.

DOI: 10.1103/PhysRevA.78.022701 PACS number(s): 34.50.Cx, 37.10.Mn, 31.70.−f, 31.50.−x

I. INTRODUCTION

There is great interest at present in producing samples of cold molecules (below 1 K) and ultracold molecules (below 1 mK). Such molecules have many potential applications. High-precision measurements on ultracold molecules might be used to measure quantities of fundamental physics interest, such as the electric dipole moment of the electron [1] and the time dependence of fundamental constants such as the electron/proton mass ratio [2]. Ultracold molecules are a stepping stone to ultracold quantum gases [3] and might have applications in quantum information and quantum computing [4].

There are two basic approaches to producing ultracold molecules. In *direct* methods such as Stark deceleration [5,6] and helium buffer-gas cooling [7], preexisting molecules are cooled from higher temperatures and trapped in electrostatic or magnetic traps. In *indirect* methods [8], laser-cooled atoms that are already ultracold are paired up to form molecules by either photoassociation [9] or tuning through magnetic Feshbach resonances [10].

Indirect methods have already been used extensively to produce ultracold molecules at temperatures below 1 μK. However, they are limited to molecules formed from atoms that can themselves be cooled to such temperatures. Direct methods are far more general than indirect methods and can in principle be applied to a very wide range of molecules. However, at present direct methods are limited to temperatures in the range 10–100 mK, which is outside the ultracold regime. There is much current research directed at finding second-stage cooling methods to bridge the gap and eventually allow directly cooled molecules to reach the region below 1 μK where quantum gases can form.

One of the most promising second-stage cooling methods that has been proposed is *sympathetic cooling*. The hope is that, if a sample of cold molecules is brought into contact with a gas of ultracold atoms, thermalization will occur and the molecules will be cooled towards the temperature of the atoms. Sympathetic cooling has already been used successfully to cool atomic species such as ^{6}Li [11] and ^{41}K [12], but has not yet been applied to neutral molecules.

Sympathetic cooling relies on thermalization occurring before molecules are lost from the trap. Thermalization requires *elastic* collisions between atoms and molecules to redistribute translational energy. However, electrostatic and magnetic traps rely on Stark and Zeeman splittings and trapped atoms and molecules are not usually in their absolute ground state in the applied field. Any *inelastic* collision that converts internal energy into translational energy is likely to kick both colliding species out of the trap. The *ratio* of elastic to inelastic cross sections is thus crucial, and a commonly stated rule of thumb is that sympathetic cooling will not work unless elastic cross sections are a factor of 10–100 greater than inelastic cross sections for the states concerned.

Inelastic cross sections for atom-atom collisions are sometimes strongly suppressed by angular momentum constraints. In particular, for *s*-wave collisions (end-over-end angular momentum $L=0$), pairs of atoms in *spin-stretched states* (with the maximum possible values of the total angular momentum F and its projection $|M_F|$) can undergo inelastic collisions only by changing L. Cross sections for such processes are very small because, for atoms in S states, the only interaction that can change L is the weak dipolar coupling between the electron spins. However, for molecular collisions the situation is different: the *anisotropy* of the intermolecular potential can change L, and this is usually much stronger than spin-spin coupling.

It is thus crucial to investigate the anisotropy of the interaction potential for systems that are candidates for sympathetic cooling experiments. In experimental terms, the easiest systems to work with are those in which molecules that can be cooled by Stark deceleration (such as NH_3, OH, and NH) interact with atoms that can be laser cooled (such as alkali-metal and alkaline-earth-metal atoms). There has been exten-

*Piotr.Zuchowski@durham.ac.uk
†J.M.Hutson@durham.ac.uk

sive work on low-energy collisions of molecules with helium atoms [13–19], but relatively little on collisions with alkali-metal and alkaline-earth-metal atoms. Soldán and Hutson [20] investigated the potential energy surfaces for Rb+NH and identified deeply bound ion-pair states as well as weakly bound covalent states. They suggested that the ion-pair states might hinder sympathetic cooling. Lara *et al.* [21,22] subsequently calculated full potential energy surfaces for Rb+OH, for both ion-pair states and covalent states, and used them to investigate low-energy elastic and inelastic cross sections, including spin-orbit coupling and nuclear spin splittings. They found that even for the covalent states the potential energy surfaces had anisotropies of the order of 500 cm^{-1} and that this was sufficient to make the inelastic cross sections larger than elastic cross sections at temperatures below 10 mK. Tacconi *et al.* [23] have recently carried out analogous calculations on Rb+NH, though without considering nuclear spin. There has also been a considerable amount of work on collisions between alkali-metal atoms and the corresponding dimers [24–29].

One way around the problem of inelastic collisions is to work with atoms and molecules that are in their absolute ground state in the trapping field. However, this is quite limiting: only optical dipole traps and alternating current traps [30] can trap such molecules. It is therefore highly desirable to seek systems in which the potential energy surface is only weakly anisotropic. The purpose of the present paper is to survey the possibilities for collision partners to use in sympathetic cooling of NH_3 (or ND_3), which is one of the easiest molecules for Stark deceleration.

Even if sympathetic cooling proves to be impractical for a particular system, the combination of laser cooling for atoms and Stark deceleration for molecules offers opportunities for studying molecular collisions in a new low-energy regime. For example, experiments are under way at the University of Colorado [31] to study collisions between decelerated NH_3 molecules and laser-cooled Rb atoms.

The energy levels of NH_3 and ND_3 are characterized by rotational quantum numbers J and K and a label $\pm$ that describes tunneling between the two equivalent umbrella configurations [32]. The molecules that can be slowed by Stark deceleration are those in states with $|K|>0$ (usually $J=1$, $|K|=1$). Both rotationally inelastic collisions and those that change the tunneling quantum number are driven by the anisotropy of the interaction potential [33,34].

The alkali-metal atom+NH_3 systems have not been extensively studied theoretically, though there has been experimental interest in the spectroscopy of Li-NH_3 as a prototype metal-atom–Lewis-base complex [35]. Lim *et al.* [36] recently calculated electrical properties and infrared spectra for complexes of NH_3 with alkali-metal atoms from K to Fr and gave the equilibrium structures of their global minima. However, to our knowledge, no complete potential energy surfaces have been published for any of these systems. The alkaline-earth-metal+NH_3 have been studied even less, and except for an early study of the Be-NH_3 system [37] there are no previous results available.

II. *Ab Initio* METHODS

The interaction energy of two monomers A and B is defined as

$$E_{\mathrm{int}}^{AB} = E_{\mathrm{tot}}^{AB} - E_{\mathrm{tot}}^{A} - E_{\mathrm{tot}}^{B} \quad (1)$$

where E_{tot}^{AB} is the total energy of the dimer and E_{tot}^{A} and E_{tot}^{B} are the total energies of the isolated monomers. Since the interaction energy is dominated at long range by intermolecular correlation (dispersion), *ab initio* calculations of the interaction energy must include electronic correlation effects at the highest possible level [38] and must be carried out with large basis sets augmented by diffuse functions. At present, the coupled-cluster (CC) method with single, double, and noniterative triple excitations [CCSD(T)] provides the best compromise between high accuracy and computational cost. In the present paper, we carry out coupled-cluster calculations using the MOLPRO package [39]. All interaction energies are corrected for basis-set superposition error (BSSE) with the counterpoise method of Boys and Bernardi [40].

Standard coupled-cluster methods are reliable only when the wave function is dominated by a single electronic configuration. This is often an issue for molecular systems with low-lying excited states. In order to check the reliability of CC calculations, it is necessary to monitor the norm of the T_1 operator [41] (measured by the T1 diagnostic). In the case of metal-NH_3 systems this is relatively large, especially when the atom approaches the lone pair of the NH_3 molecule, but the convergence of the CC equations is fast and converged CCSD results are very close to benchmark multireference configuration interaction (MRCI-SD) calculations with size-extensivity corrections. Thus we consider CC results reliable.

To understand the origin of the intermolecular forces we also consider the interaction energies obtained at the Hartree-Fock level, which neglects electron correlation. The comparison between Hartree-Fock and coupled-cluster results thus provides information about the role of dispersion and other correlation effects. For some systems we also analyze the components of the intermolecular interactions using symmetry-adapted perturbation theory [42] (SAPT). The first-order SAPT corrections (electrostatic and exchange terms) are computed from Hartree-Fock monomer wave functions, while the dispersion energy is evaluated with the coupled Hartree-Fock approach [43] without full spin adaptation. These calculations are carried out using the SAPT2006 [44] program.

We are interested principally in the collisions of cold ammonia molecules with atoms at energies that are much too low for vibrational excitation to occur. Such collisions are governed by an effective potential that is vibrationally averaged over the ground-state vibrational wave function of NH_3. For the present purpose it is adequate to represent this by a potential calculated with the NH_3 molecule frozen at a geometry that represents the ground state. In the present paper we use a geometry derived from the high-resolution infrared spectra [45]: the molecule is taken to have C_{3v} symmetry with N-H bond lengths of $1.913a_0$ and an H-N-H angle of 106.7°. Intermolecular geometries are specified in Jacobi coordinates: R is the distance from the center of mass of NH_3 to the atom, while θ is the angle between the intermolecular vector and the C_3 axis of the NH_3 molecule (with $\theta=0°$ corresponding to the atom approaching towards the lone pair

TABLE I. Properties of alkali-metal, alkaline-earth-metal, and Xe atoms important to interaction potentials. Note that for alkali-metal atoms the lowest excitation energy corresponds to $^2S \rightarrow {}^2P_{1/2}$ excitation and for alkaline-earth-metal and Xe atoms to $^1S \rightarrow {}^3P_0$. The excitation and ionization energies are taken from [46].

Atom	dipole polarizability (units of a_0^3)	Ref.	Lowest excitation energy (cm^{-1})	Ionization energy (cm^{-1})	C_6 coefficient (units of $E_h a_0^6$)	Ref.
Li	164	[47]	14904	43487	1395	[48]
Na	162	[49]	16956	41449	1561	[48]
K	293	[49]	12985	35010	3921	[50]
Rb	319	[49]	12578	33691	4707	[51]
Be	37.7	[48]	21978	75193	213	[48]
Mg	71	[48]	21850	61671	629	[48]
Ca	159	[48]	15157	49305	2221	[52]
Sr	200	[48]	14317	45932	3250	[48]
Xe	27.3	[53]	67068	97834	286	[54]

of NH_3). Finally, χ is the dihedral angle between the plane containing the C_3 axis and an NH bond and that containing the C_3 axis and the intermolecular vector.

Table I gives the lowest excitation energies, dipole polarizabilities, and ionization energies of the atoms studied in this paper. The neutral alkali-metal and alkaline-earth-metal atoms (denoted below as A and Ae, respectively) have particularly low excitation energies, resulting from small separations between energy levels corresponding to ns and np or $(n-1)d$ configurations. Since the gap between the ground and excited states is small, the atoms have very large polarizabilities. Hence, we expect particularly strong induction and dispersion interactions. The alkali-metal and alkaline-earth-metal atoms also have low ionization energies E_i. Since the atomic orbital wave functions vanish at long range as $\exp(-E_i^{1/2}r)$, the wave functions and densities are very diffuse, and this causes a large overlap between monomers even at relatively large separations. Finally, because of the low ionization energies, alkali-metal and alkaline-earth-metal atoms have a strong tendency to form charge-transfer complexes.

The basis sets used in the *ab initio* calculations are as follows. For Be, Li, Mg, Na, and Ca atoms we use all-electron cc-pVTZ basis sets [55] (correlation-consistent polarized valence triple-zeta) augmented by even-tempered diffuse exponents, while for potassium we use the correlation-valence CVTZ basis set of Feller *et al.* [56]. For Rb, Sr, and Xe we handle only the outermost electrons explicitly, with the core electrons represented by effective core potentials (ECPs). For Rb we use the small-core effective core potential ECP28MWB with a basis set based on that of Ref. [57], which was optimized to recover the static dipole polarizability. We modified this slightly to account better for intramonomer electronic correlation effects by removing 0.07 f and adding 0.001049 s, 0.0024 p, 4.5 and 0.016667 d, 1.9 and 0.655 f, and 0.95 and 0.3167 g functions. The basis set for Sr is taken from Ref. [58]. For Xe we use the basis set given by Lozeille *et al.* [53], which was found to be excellent for polarizabilities and hyperpolarizabilities. For each system we added a set of midbond functions with exponents sp: 0.9,0.3,0.1, df: 0.6,0.2 to improve the representation of the dispersion energy in the region of the van der Waals minimum.

III. RESULTS AND DISCUSSION

The potential energy surface for an atom-NH_3 system is a function of the intermolecular distance R and two angles θ and χ. However, functions of three variables are difficult to represent graphically. It is convenient to represent the χ dependence in the form

$$V(R,\theta,\chi) = \sum_{k=0}^{\infty} V_{3k}(R,\theta)\cos 3k\chi. \tag{2}$$

To reduce the computational effort we calculate the interaction potential only for $\chi=0°$ and $\chi=60°$ and approximate the leading terms $V_0(R,\theta)$ and $V_3(R,\theta)$ by sum and difference potentials,

$$V_0(R,\theta) = \frac{1}{2}[V(R,\theta,0°) + V(R,\theta,60°)]$$

$$V_3(R,\theta) = \frac{1}{2}[V(R,\theta,0°) - V(R,\theta,60°)]. \tag{3}$$

V_0 can be viewed as the interaction potential averaged over χ, while V_3 describes the variation of the potential with respect to rotation about the C_3 axis of NH_3; V_3 is referred to below as the noncylindrical term.

A. Alkali-metal atom+NH_3 interactions

The potential energy surface for Rb-NH_3 is shown in Fig. 1. CCSD(T) calculations were carried out at $\chi=0°$ and 60°, at values of θ corresponding to a 20-point Gauss-Lobatto quadrature. The grid included R values from $3.5a_0$ to $12a_0$ with a step of $0.5a_0$ and from $12a_0$ to $15a_0$ with a step of $1a_0$. There is a deep minimum (1862 cm^{-1}) at $R=5.90a_0$ and $\theta=0°$, corresponding to approach of Rb towards the NH_3 lone

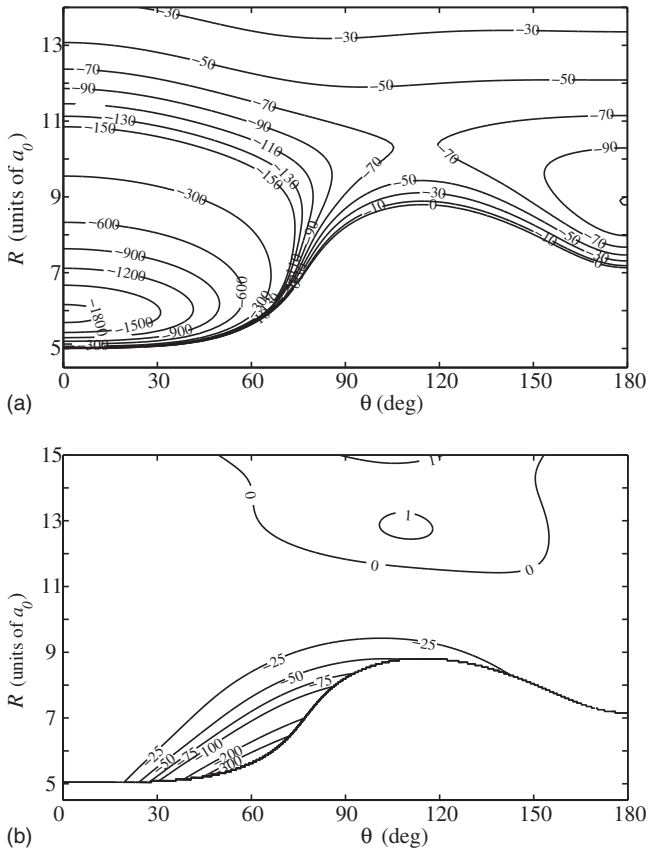

FIG. 1. The interaction potential of Rb-NH_3 from CCSD(T) calculations: $V_0(R,\theta)$ component (upper panel) and $V_3(R,\theta)$ component (lower panel). Contours are labeled in cm^{-1}. To aid visualization, V_3 is plotted only in the energetically accessible region defined by $V_0<0$.

pair. The potential is much shallower at other geometries, with a saddle point near $\theta=110°$ and a shallow secondary minimum at $\theta=180°$. The noncylindrical term $V_3(R,\theta)$ is relatively weak, at least in the low-energy classically allowed region defined by $V_0(R,\theta)<0$.

The overall shape of the other A-NH_3 potentials is quite similar. In each case there is a deep minimum around $\theta=0°$ and a shallow secondary minimum for $\theta=180°$. Table II gives the well depths and equilibrium distances. For the alkali metals the well depth of the global minimum decreases down the periodic table, from 5104 cm^{-1} for Li to 1862 cm^{-1} for Rb, and the equilibrium distance increases from $3.91a_0$ for Li to $5.90a_0$ for Rb. The changes in the properties of the

TABLE II. Equilibrium distances and well depths for alkali-metal atom+NH_3 systems from CCSD(T) calculations.

	$\theta=0°$		$\theta=180°$	
	R_e (units of a_0)	D_e (cm^{-1})	R_e (units of a_0)	D_e (cm^{-1})
Li	3.91	5104	7.86	104.8
Na	4.73	2359	8.33	98.2
K	5.52	2161	8.90	99.6
Rb	5.90	1862	8.89	110.2

TABLE III. Equilibrium distances and well depths for alkaline-earth-metal atom+NH_3 systems from CCSD(T) calculations.

	$\theta=0°$		$\theta=180°$	
	R_e (units of a_0)	D_e (cm^{-1})	R_e (units of a_0)	D_e (cm^{-1})
Be	3.57	1973	7.61	100.5
Mg	4.83	887.5	8.20	115.7
Ca	4.92	3229	8.85	129.1
Sr	5.22	3141	9.06	131.6

shallow secondary minima are much smaller, with well depths close to 100 cm^{-1} for all the alkali metals. Our results for the species containing K and Rb are in good agreement with the CCSD(T) calculations of Lim *et al.* [36]; they obtained slightly different values of the binding energies of K-NH_3 and Rb-NH_3 (2210 cm^{-1} and 1950 cm^{-1}, respectively), but their results are not corrected for BSSE. It should also be noted that their binding energies are for relaxed NH_3 geometries.

The deep wells and large anisotropies of the A-NH_3 potentials will produce strong coupling between the different NH_3 rotational and inversion states during collisions. All these systems are therefore likely to have large inelastic cross sections. It is thus unlikely that sympathetic cooling of NH_3 with alkali-metal atoms will be successful unless both the atoms and the molecules are already in their lowest internal states for the symmetry concerned.

B. Alkaline-earth-metal atom+NH_3 interactions

We originally hoped that the potentials for systems containing alkaline-earth-metal atoms would be more weakly bound and less anisotropic than for those containing alkali-metal atoms. However, this proved not to be the case, at least for the heavier alkaline-earth-metal atoms that are most suitable for laser cooling. The results for the Ae-NH_3 systems are summarized in Table III. The shapes of the potential energy surfaces are generally similar to those for A-NH_3 systems. For Ca and Sr, the depths of the global minima are 3229 and 3141 cm^{-1} respectively; these are both deeper than for the corresponding alkali-metal atom. For Mg, however, the well depth is considerably shallower at only 887.5 cm^{-1}. The minima corresponding to approach at the hydrogen end of NH_3 are slightly deeper than for the alkali metals, ranging from 115.7 for Mg to 131.6 cm^{-1} for Sr. On the other hand, the interaction potential for Be-NH_3 resembles those for Ca-NH_3 and Sr-NH_3 more than that for Mg-NH_3: the global minimum is 1973 cm^{-1} deep, while the dispersion-bound minimum is 100.5 cm^{-1} deep. The equilibrium distance for Be-NH_3 at $\theta=0°$ ($3.57a_0$) is also much shorter than for the other Ae-NH_3 systems and is comparable to that for Li-NH_3.

C. Origin of bonding in metal-atom+NH_3 systems

It is important to understand the large difference between the metal-lone-pair bond energies between Mg and the other group-1 and -2 atoms considered here. Table IV gives

TABLE IV. The interaction energies (in cm^{-1}) for Li-NH_3, Ca-NH_3, and Mg-NH_3 at different levels of electronic correlation, for geometries corresponding to the CCSD(T) global and secondary minima.

	Global minimum			Secondary minimum		
	HF	CCSD	CCSD(T)	HF	CCSD	CCSD(T)
Li	−4405	−5022	−5104	248	−54	−105
Ca	−2152	−2937	−3229	244	−47	−129
Mg	260	−590	−888	155	−54	−116

the interaction energies at the Hartree-Fock, CCSD, and CCSD(T) levels at the positions of the CCSD(T) global and secondary minima for Li-NH_3, Mg-NH_3, and Ca-NH_3. For all these systems the Hartree-Fock interaction energies are positive for the shallow secondary minima, indicating that the shallow wells are dominated by dispersion forces. At the global minima, however, Mg-NH_3 is repulsive at the Hartree-Fock level while the other two systems are strongly attractive. There is thus strong chemical bonding in Li-NH_3 and Ca-NH_3 that is absent in Mg-NH_3.

The qualitative differences between Mg and the other atoms can be understood if we consider how the energy of the highest occupied molecular orbital (HOMO) differs for the different atom-NH_3 systems. Figure 2 shows the two highest occupied molecular orbitals of each system. As we separate the monomers to infinity, these two orbitals became HOMOs of the atom and the NH_3 molecule. For any alkali-metal atom, the strong A-NH_3 bond can be explained as a chemical bond of order one-half, since we have a doubly occupied bonding orbital and a singly occupied antibonding orbital [see Fig. 2(a)]. However, this explanation does not apply to the alkaline-earth-metal atoms, where the antibonding orbital is doubly occupied. The net bonding in Ca-NH_3 arises because the bonding orbital is shifted down in energy considerably more than the antibonding orbital is shifted up. Conversely, in Mg-NH_3, the contributions from the bonding and antibonding orbitals are closely balanced. The difference can probably be attributed to the participation of np orbitals; as shown in Table I, the $S \rightarrow P$ splitting is considerably smaller

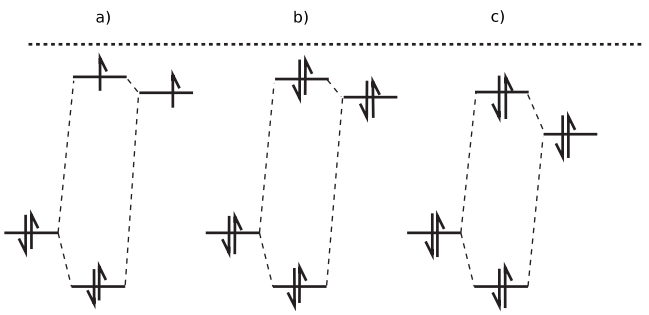

FIG. 2. The pattern of molecular orbitals for (a) Li-NH_3, (b) Ca-NH_3, and (c) Mg-NH_3 near their global minima. The HOMOs of NH_3 and of the metal atoms form bonding and antibonding orbitals. Note the small change in the HOMO energy for the Li-NH_3 and Ca-NH_3 systems and the much larger change for Mg-NH_3.

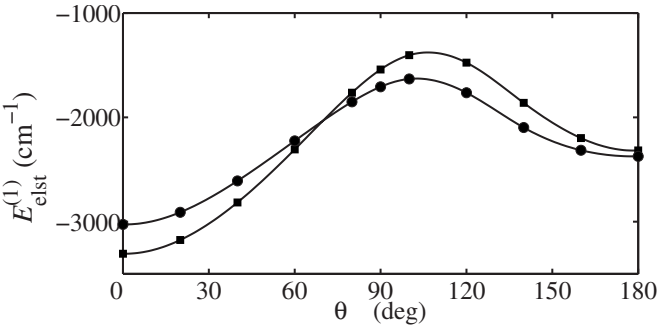

FIG. 3. Electrostatic contribution to $V_0(R,\theta)$ for Na-NH_3 (squares) and Mg-NH_3 (circles) for $R=6a_0$.

in Ca than in Mg. Thus Mg-NH_3 is bound mainly by dispersion forces whereas Ca-NH_3 has substantial chemical bonding.

Different considerations apply to the Be atom, which is a notoriously difficult case for electronic structure theory [59]. Although the potential energy surfaces are qualitatively similar for the Be-NH_3, Ca-NH_3, and Sr-NH_3 systems at the CCSD(T) level, the origin of the strong bonding is probably different in Be-NH_3. In this case the Hartree-Fock and CCSD potential energy curves for $\theta=0°$ show a double-minimum structure, with a shallow long-range minimum separated from the global minimum by a barrier. This suggests a sudden change in chemical character as the Be atom approaches N. At the Hartree-Fock level the maximum has an energy of 730 cm^{-1} at $R=4.88a_0$. The long-range minimum at the Hartree-Fock level is 18.4 cm^{-1} deep at $R=9.02a_0$, while at the CCSD level it is 138 cm^{-1} deep at $R=6.5a_0$. Despite this peculiar behavior, the CC calculations showed no convergence problems or unusually large T1 diagnostics. However, our results for Be-NH_3 disagree with those of Chałasiński and co-workers [37], who carried out fourth-order Moller-Plesset (MP4) calculations and found a global minimum that corresponds to the outer minimum on the CCSD potential energy curve. They did not find the inner minimum, which turned out to be the global minimum in our calculations.

As mentioned before, the feature of the potential energy surfaces that is important for elastic and inelastic collision ratios is the anisotropy. In order to understand the origin of the anisotropies better, we carried out additional calculations based on SAPT. Figures 3–5 show the electrostatic, first-order exchange, and dispersion components of the interaction energy V_0 for Na-NH_3 and Mg-NH_3, averaged over χ as in Eq. (3). The calculations were performed at a fixed R value of $6a_0$, which is in an attractive region for $\theta=0°$ and a repulsive region for $\theta=180°$. Figures 3–5 show clearly that it is the first-order interaction energy that is responsible for most of the anisotropy in the valence overlap region. This is caused by a very large difference between the electrostatic attraction near the lone-pair site and near hydrogen sites (see Fig. 3). This difference is significantly larger than that in the exchange energy. The anisotropy of the dispersion interaction (plotted in Fig. 5), is even weaker.

The three components of V_3 are shown for Na-NH_3 and Mg-NH_3 in Fig. 6. The exchange energy is very strongly

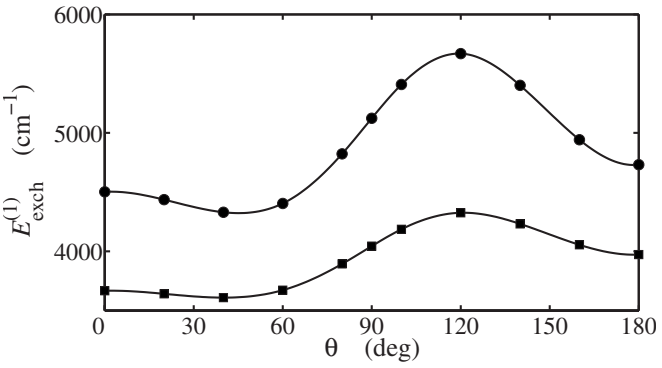

FIG. 4. First-order exchange contribution to $V_0(R,\theta)$ for Na-NH_3 (squares) and Mg-NH_3 (circles) for $R=6a_0$.

noncylindrical, especially for Mg-NH_3. The large difference in the exchange component between Mg-NH_3 and Na-NH_3 can be explained by the closed-shell character of the Mg atom and the much stronger Pauli repulsion between hydrogens of NH_3 and Mg. The electrostatic and dispersion contributions to V_3 are much more similar for the two systems.

D. Xe+NH_3 interaction

The potential energy surfaces for all the metal-NH_3 systems investigated above have disappointingly large anisotropies. It is likely that all these systems will exhibit large inelastic cross sections for any initial state where inelasticity is possible. We therefore decided to consider other possible collision partners for sympathetic cooling of NH_3. Barker [60] has suggested an experiment in which Xe is first laser cooled in its metastable $^3P_2$ state and then transferred to its ground $^1S_0$ state by laser excitation followed by spontaneous emission. Since ground-state Xe has a fairly large dipole polarizability, it can be held in an optical dipole trap and might be used for sympathetic cooling. In this subsection we investigate the Xe-NH_3 interaction in order to evaluate its potential in this respect.

Interactions between noble gases and ammonia have been studied extensively. The interaction between He and NH_3 is important in understanding the spectroscopy of NH_3 molecules in helium nanodroplets [61]. The most recent *ab initio* calculations of Hodges and Wheatley [62,63] gave a global minimum about 33 cm^{-1} deep at $R=6a_0$, $\theta=90°$, and $\chi=60°$. The interaction of Ar with NH_3 has been studied even more extensively, both experimentally [64] and by *ab initio* methods [65,66]. Inversion of vibration-rotation-tunneling spectra [64] gave a minimum 147 cm^{-1} deep at $R=6.5a_0$, $\theta=97°$, and $\chi=60°$, while the *ab initio* MP4 (fourth-order Møller-Plesset) calculations of Tao and Klemperer [66] gave a global minimum 130 cm^{-1} deep at $R=6.85a_0$, $\theta=90°$, and $\chi=60°$. The Ne-NH_3 system was investigated through MP4 calculations by van Wijngaarden and Jäger [67], who obtained a global minimum 63 cm^{-1} deep at $R=6.1a_0$, $\theta=90°$, and $\chi=60°$. For Kr-NH_3, Chałasiński *et al.* [68] obtained a global minimum 108 cm^{-1} deep at $R=7.2a_0$, $\theta=100°$, and $\chi=60°$. However, their results were based on calculations at the MP2 level and may not reproduce the dispersion energy accurately.

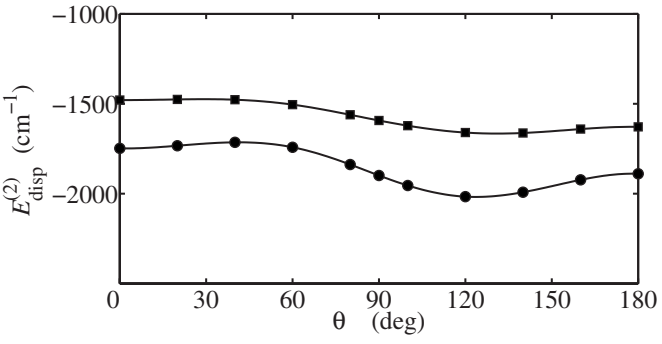

FIG. 5. Dispersion contribution to $V_0(R,\theta)$ for Na-NH_3 (squares) and Mg-NH_3 (circles) for $R=6a_0$.

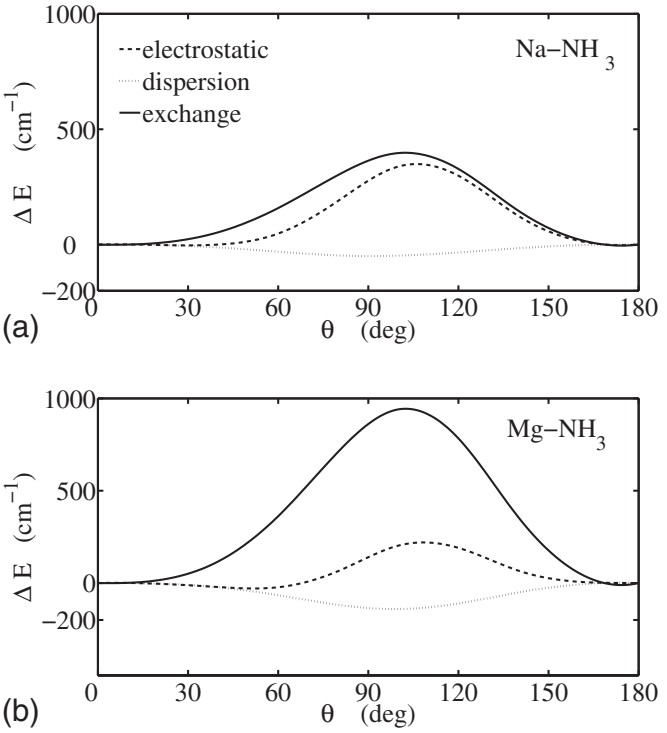

FIG. 6. Components of $V_3(R,\theta)$ for Na-NH_3 (upper panel) and Mg-NH_3 (lower panel) for $R=6a_0$.

Figure 7 shows the interaction potential for Xe-NH_3 from our CCSD(T) calculations. The potential energy surface differs qualitatively from those for metal-NH_3 potentials studied in the previous subsection and behaves analogously to those for other Rg-NH_3 systems. The V_0 surface for Xe-NH_3 has only one minimum, 173.5 cm^{-1} deep, at $R=7.65a_0$ and $\theta=66°$. The global minimum for the nonexpanded surface is 196.8 cm^{-1} deep, at $R=7.35a_0$, $\theta=81°$, and $\chi=60°$. There are saddle points at both C_{3v} configurations. For $\theta=0$ the saddle point is 166.2 cm^{-1} deep at $R=7.73a_0$, while for $\theta=180°$ the saddle point is 134.1 cm^{-1} deep at $R=7.93a_0$. The major binding arises from the dispersion energy, and at the Hartree-Fock level we observe only a small attraction (a few cm^{-1}) at large distances, due to weak induction forces which behave asymptotically as $-C_6R^{-6}$. Near the van der Waals minimum predicted by CCSD(T), the Hartree-Fock energy is repulsive.

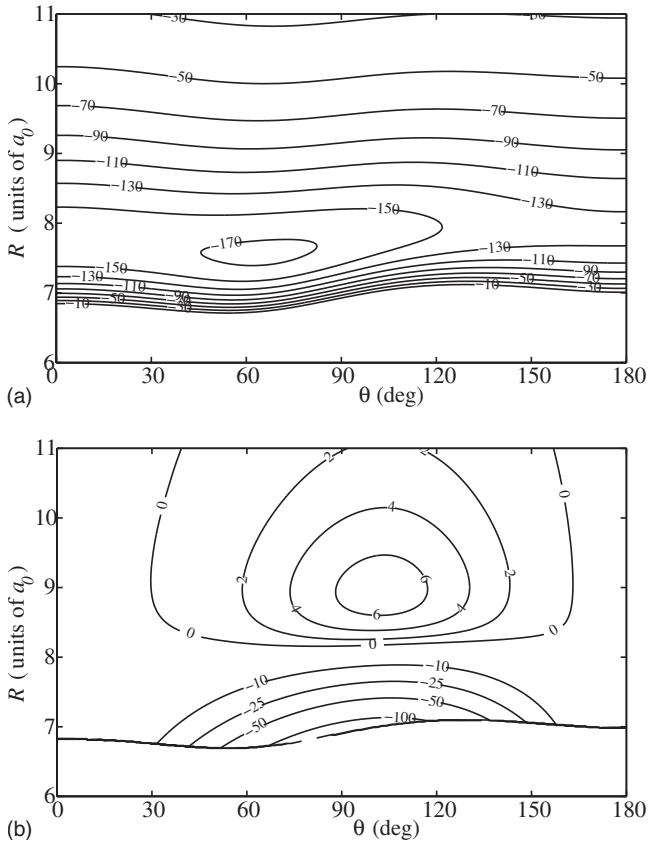

FIG. 7. The interaction potential of Xe-NH_3 from CCSD(T) calculations: $V_0(R,\theta)$ component (upper panel) and $V_3(R,\theta)$ component (lower panel). Contours are labeled in cm^{-1}. To aid visualization, V_3 is plotted only in the energetically accessible region defined by $V_0<0$.

The V_0 surface for Xe-NH_3 system thus has an anisotropy of only about 60 cm^{-1} between the potential minimum and the higher of the two saddle points. This is considerably smaller than for Rb-OH or any of the metal-NH_3 systems studied here, but still substantial compared to the rotational constant of NH_3, $b=6.35$ cm^{-1} for rotation about an axis perpendicular to C_3.

E. Long-range forces

Long-range forces are very important in cold and ultracold collisions. We therefore carried out separate calculations of the van der Waals coefficients for the interactions. The isotropic $C_{6,0}$ and anisotropic $C_{6,2}$ dispersion coefficients for the interaction of atom A and symmetric top molecule B may be written in terms of the dynamic polarizabilities of the monomers, evaluated at imaginary frequencies [69],

$$C_{6,0}^{\mathrm{disp}} = \frac{3}{\pi}\int_0^{+\infty} \alpha_A(iu)\bar{\alpha}_B(iu)du,$$

$$C_{6,2}^{\mathrm{disp}} = \frac{1}{\pi}\int_0^{+\infty} \alpha_A(iu)\Delta\alpha_B(iu)du, \qquad (4)$$

where $\bar{\alpha}=\frac{1}{3}(2\alpha_{xx}+\alpha_{zz})$ is the isotropic polarizability and $\Delta\alpha=\alpha_{zz}-\alpha_{xx}$ is the polarizability anisotropy. The induction contributions to the van der Waals coefficients are

$$C_{6,0}^{\mathrm{ind}} = C_{6,2}^{\mathrm{ind}} = \alpha_A\mu^2, \qquad (5)$$

where the dipole moment μ is $0.579ea_0$ for NH_3 [70].

TABLE V. Van der Waals dispersion and induction coefficients for A-NH_3 and Ae-NH_3 systems. All values are in atomic units, $E_h a_0^6$.

	$C_{6,0}^{\mathrm{disp}}$	$C_{6,2}^{\mathrm{disp}}$	$C_{6,0}^{\mathrm{ind}}=C_{6,2}^{\mathrm{ind}}$
Li	224	7.2	55.0
Na	258	7.4	54.3
K	378	11.6	98.2
Rb	416	12.5	106.9
Be	121	2.3	12.7
Mg	200	4.4	24.0
Ca	342	8.4	53.4
Sr	413	10.2	67.4
Xe	161	0.94	9.1

The integrals in Eqs. 4 were evaluated using the method given by Amos *et al.* [71]. The dynamic polarizabilities of NH_3 were obtained using coupled Kohn-Sham theory with the asymptotically corrected PBE0 functional [72] and doubly augmented d-aug-cc-pVTZ basis sets [55]. To get the dynamic polarizabilities for the alkali-metal atoms, we adjusted the fraction of exchange, exact exchange, and correlation fraction in the PBE0 functional in such a way as to recover the atom-atom C_6 coefficients (see Table I). Our coupled Kohn-Sham program does not allow us to use core potentials to calculate dynamic polarizabilities. For Rb we therefore performed all-electron calculations with the pVTZ basis set of Sadlej [73] combined with the Douglas-Kroll approximation [74]. The dynamic polarizabilities obtained in this way were tested by comparing C_6 coefficients for A-Ar and A-Xe systems with those obtained by Mitroy and Zhang [75]. The maximum error was found to be +6.3% (for Na-Xe) while the average error is less than +3%. For alkaline-earth-metal and Xe atoms the frequency-dependent dipole polarizabilities were obtained from time-independent coupled-cluster linear response functions [76,77].

The resulting C_6 coefficients are shown in Table V. For the alkali-metal and alkaline-earth-metal atoms, the isotropic dispersion coefficients $C_{6,0}^{\mathrm{disp}}$ are fairly large because of the large atomic polarizabilities. The anisotropies in the dispersion coefficients are much smaller, because of the small polarizability anisotropy of NH_3 ($2.1a_0^3$) compared to its isotropic polarizability ($14.6a_0^3$). The induction van der Waals coefficients are large and account for 10%–25% of the total $C_{6,0}$ and 70%–90% of the total $C_{6,2}$. It may be noted that $C_{6,0}^{\mathrm{disp}}$ for Rb-NH_3 is somewhat larger than $C_{6,00}^{\mathrm{disp}}$ for Rb-OH [22]. As one might expect, the Xe-NH_3 long-range interaction has slightly different character from the A- and Ae-NH_3 systems. The $C_{6,0}^{\mathrm{disp}}$ coefficient is still large, but the total anisotropy (in particular the dispersion anisotropy) is much smaller.

IV. CONCLUSIONS

We have investigated the intermolecular potential energy surfaces for interaction of NH_3 with several different atoms that might be used for sympathetic cooling. Both rotationally inelastic collisions and those that change the tunneling quantum number are governed by the anisotropy of the interaction potential. For interaction with all the alkali-metal and alkaline-earth-metal atoms, we found deep minima and strong anisotropies. The shallowest potential is for Mg-NH_3, but even there the anisotropy in the well depth is close to 800 cm^{-1}. This is likely to cause strong inelastic collisions for all initial states for which they are energetically and symmetry allowed. Accordingly, we consider that none of the alkali metals and alkaline earth metals are good prospects for sympathetic cooling of NH_3 unless both the atoms and the molecules are in their lowest states in the trapping field for the symmetry concerned. This suggests that sympathetic cooling would need to be carried out in either optical or alternating current traps.

A somewhat more promising system for sympathetic cooling is Xe-NH_3, for which the global minimum is calculated to be 196.8 cm^{-1} deep at an off-axis geometry. The Xe-NH_3 system is relatively weakly anisotropic, with the saddle points for C_{3v} geometries only 30.6 and 62.7 cm^{-1} higher than the global minimum. In future work we will use the interaction potential to calculate low-energy elastic and inelastic cross sections, in order to predict whether sympathetic cooling of NH_3 by Xe is likely to be feasible.

Even if sympathetic cooling proves to be impossible for these systems, there is much to be learnt from collisions between velocity-controlled beams of molecules and laser-cooled atoms. There are opportunities to explore low-energy inelastic processes in novel collisional regimes and to probe scattering resonances in unprecedented detail. We therefore intend to use the potential energy surfaces developed here to carry out inelastic collision calculations to explore these effects and assist in the interpretation of collision experiments.

ACKNOWLEDGMENTS

The authors are grateful to EPSRC for funding of the collaborative project CoPoMol under the ESF EUROCORES Programme EuroQUAM.

[1] J. J. Hudson, B. E. Sauer, M. R. Tarbutt, and E. A. Hinds, Phys. Rev. Lett. **89**, 023003 (2002).
[2] J. van Veldhoven, J. Küpper, H. L. Bethlem, B. Sartakov, A. J. A. van Roij, and G. Meijer, Eur. Phys. J. D **31**, 337 (2004).
[3] M. Baranov, Ł. Dobrek, K. Góral, L. Santos, and M. Lewenstein, Phys. Scr. **T102**, 74 (2002).
[4] D. DeMille, Phys. Rev. Lett. **88**, 067901 (2002).
[5] H. L. Bethlem and G. Meijer, Int. Rev. Phys. Chem. **22**, 73 (2003).
[6] H. L. Bethlem, M. R. Tarbutt, J. Küpper, D. Carty, K. Wohlfart, E. A. Hinds, and G. Meijer, J. Phys. B **39**, R263 (2006).
[7] J. D. Weinstein, R. deCarvalho, T. Guillet, B. Friedrich, and J. M. Doyle, Nature (London) **395**, 148 (1998).
[8] J. M. Hutson and P. Soldán, Int. Rev. Phys. Chem. **25**, 497 (2006).
[9] K. M. Jones, E. Tiesinga, P. D. Lett, and P. S. Julienne, Rev. Mod. Phys. **78**, 483 (2006).
[10] T. Köhler, K. Goral, and P. S. Julienne, Rev. Mod. Phys. **78**, 1311 (2006).
[11] F. Schreck, G. Ferrari, K. L. Corwin, J. Cubizolles, L. Khaykovich, M. O. Mewes, and C. Salomon, Phys. Rev. A **64**, 011402(R) (2001).
[12] G. Modugno, G. Ferrari, G. Roati, R. J. Brecha, A. Simoni, and M. Inguscio, Science **294**, 1320 (2001).
[13] N. Balakrishnan, R. C. Forrey, and A. Dalgarno, Chem. Phys. Lett. **280**, 1 (1997).
[14] N. Balakrishnan, R. C. Forrey, and A. Dalgarno, Astrophys. J. **514**, 520 (1999).
[15] N. Balakrishnan, A. Dalgarno, and R. C. Forrey, J. Chem. Phys. **113**, 621 (2000).
[16] J. L. Bohn, Phys. Rev. A **62**, 032701 (2000).
[17] N. Balakrishnan, G. C. Groenenboom, R. V. Krems, and A. Dalgarno, J. Chem. Phys. **118**, 7386 (2003).
[18] R. V. Krems, H. R. Sadeghpour, A. Dalgarno, D. Zgid, J. Kłos, and G. Chałasiński, Phys. Rev. A **68**, 051401(R) (2003).
[19] M. L. González-Martínez and J. M. Hutson, Phys. Rev. A **75**, 022702 (2007).
[20] P. Soldán and J. M. Hutson, Phys. Rev. Lett. **92**, 163202 (2004).
[21] M. Lara, J. L. Bohn, D. Potter, P. Soldán, and J. M. Hutson, Phys. Rev. Lett. **97**, 183201 (2006).
[22] M. Lara, J. L. Bohn, D. E. Potter, P. Soldán, and J. M. Hutson, Phys. Rev. A **75**, 012704 (2007).
[23] M. Tacconi, L. Gonzalez-Sanchez, E. Bodo, and F. A. Gianturco, Phys. Rev. A **76**, 032702 (2007).
[24] P. Soldán, M. T. Cvitaš, J. M. Hutson, P. Honvault, and J. M. Launay, Phys. Rev. Lett. **89**, 153201 (2002).
[25] G. Quéméner, P. Honvault, and J. M. Launay, Eur. Phys. J. D **30**, 201 (2004).
[26] M. T. Cvitaš, P. Soldán, J. M. Hutson, P. Honvault, and J. M. Launay, Phys. Rev. Lett. **94**, 033201 (2005).
[27] M. T. Cvitaš, P. Soldán, J. M. Hutson, P. Honvault, and J. M. Launay, Phys. Rev. Lett. **94**, 200402 (2005).
[28] G. Quéméner, P. Honvault, J. M. Launay, P. Soldán, D. E. Potter, and J. M. Hutson, Phys. Rev. A **71**, 032722 (2005).
[29] J. M. Hutson and P. Soldán, Int. Rev. Phys. Chem. **26**, 1 (2007).
[30] J. van Veldhoven, H. L. Bethlem, and G. Meijer, Phys. Rev. Lett. **94**, 083001 (2005).
[31] H. J. Lewandowski (private communication).
[32] G. Herzberg, *Infrared and Raman Spectra* (Van Nostrand, Princeton, 1945).
[33] S. L. Davis and J. E. Boggs, J. Chem. Phys. **69**, 2355 (1978).
[34] S. Green, J. Chem. Phys. **73**, 2740 (1980).
[35] J. Wu, M. J. Polce, and C. Wesdemiotis, Int. J. Mass. Spectrom. **204**, 125 (2001).

[36] I. S. Lim, P. Botschwina, R. Oswald, V. Barone, H. Stoll, and P. Schwerdtfeger, J. Chem. Phys. **127**, 104313 (2007).
[37] G. Chalasinski, M. M. Szczesniak, and S. Scheiner, J. Chem. Phys. **98**, 7020 (1993).
[38] G. Chalasinski and M. M. Szczesniak, Chem. Rev. (Washington, D.C.) **100**, 4227 (2000).
[39] H.-J. Werner, P. J. Knowles, R. Lindh, M. Schütz *et al.*, Computer code MOLPRO, version 2002.6, a package of *ab initio* programs, 2003; see http://www.molpro.net
[40] S. F. Boys and F. Bernardi, Mol. Phys. **19**, 553 (1970).
[41] T. J. Lee and P. R. Taylor, Int. J. Quantum Chem. **S23**, 199 (1989).
[42] B. Jeziorski, R. Moszynski, and K. Szalewicz, Chem. Rev. (Washington, D.C.) **94**, 1887 (1994).
[43] P. S. Żuchowski, B. Bussery-Honvault, R. Moszynski, and B. Jeziorski, J. Chem. Phys. **119**, 10497 (2003).
[44] R. Bukowski, W. Cencek, P. Jankowski, M. Jeziorska, B. Jeziorski, V. F. Lotrich, S. A. Kucharski, A. J. Misquitta, R. Moszyński, K. Patkowski *et al.*, Computer code SAPT2006.1: an *ab initio* program for many-body symmetry-adapted perturbation theory calculations of intermolecular interaction energies, University of Delaware and University of Warsaw, 2006, http://www.physics.udel.edu/~szalewic/SAPT/SAPT.html
[45] W. S. Benedict, N. Gailar, and E. K. Plyler, Can. J. Phys. **35**, 1235 (1957).
[46] J. E. Sansonetti, W. C. Martin, and S. Young, *Handbook of Basic Atomic Spectroscopic Data*, version 1.1.2 (National Institute of Standards and Technology, Gaithersburg, MD, 2005); http://physics.nist.gov/PhysRefData/Handbook
[47] Z. C. Yan, J. F. Babb, A. Dalgarno, and G. W. F. Drake, Phys. Rev. A **54**, 2824 (1996).
[48] J. Mitroy and M. W. J. Bromley, Phys. Rev. A **68**, 052714 (2003).
[49] U. Volz and H. Schmoranzer, Phys. Scr. **T65**, 44 (1996).
[50] A. Pashov, P. Popov, H. Knöckel, and E. Tiemann, Eur. Phys. J. D **46**, 241 (2008).
[51] A. Marte, T. Volz, J. Schuster, S. Durr, G. Rempe, E. G. M. van Kempen, and B. J. Verhaar, Phys. Rev. Lett. **89**, 283202 (2002).
[52] S. G. Porsev and A. Derevianko, Phys. Rev. A **65**, 020701(R) (2002).
[53] J. Lozeille, E. Winata, P. Soldán, E. F. Lee, L. A. Viehland, and T. G. Wright, Phys. Chem. Chem. Phys. **4**, 3601 (2002).
[54] K. T. Tang and J. P. Toennies, J. Chem. Phys. **118**, 4976 (2003).
[55] EMSL basis set exchange at https://bse.pnl.gov/bse/portal.
[56] D. Feller, E. D. Glendening, D. E. Woon, and M. W. Feyereisen, J. Chem. Phys. **103**, 3526 (1995).
[57] P. Soldán, M. T. Cvitaš, and J. M. Hutson, Phys. Rev. A **67**, 054702 (2003).
[58] I. S. Lim, H. Stoll, and P. Schwerdtfeger, J. Chem. Phys. **124**, 034107 (2006).
[59] K. Patkowski, R. Podeszwa, and K. Szalewicz, J. Phys. Chem. A **111**, 12822 (2007).
[60] P. F. Barker (private communication).
[61] M. Behrens, U. Buck, R. Fröchtenicht, M. Hartmann, F. Huisken, and F. Rohmund, J. Chem. Phys. **109**, 5914 (1998).
[62] Z. Li, A. Chou, and F.-M. Tao, Chem. Phys. Lett. **313**, 313 (1999).
[63] M. P. Hodges and R. J. Wheatley, J. Chem. Phys. **114**, 8836 (2001).
[64] C. A. Schmuttenmaer, R. C. Cohen, and R. J. Saykally, J. Chem. Phys. **101**, 146 (1994).
[65] G. Chalasinski, M. M. Szczesniak, and S. Scheiner, J. Chem. Phys. **91**, 7809 (1989).
[66] F.-M. Tao and W. Klemperer, J. Chem. Phys. **101**, 1129 (1994).
[67] J. van Wijngaarden and W. Jäger, J. Chem. Phys. **115**, 6504 (2001).
[68] G. Chalasinski, M. M. Szczesniak, and S. Schneier, J. Chem. Phys. **97**, 8181 (1992).
[69] A. J. Stone, *The Theory of Intermolecular Forces* (Oxford University Press, Oxford, 1996).
[70] C. A. Schmuttenmaer, R. C. Cohen, J. G. Loeser, and R. J. Saykally, J. Chem. Phys. **95**, 9 (1991).
[71] R. D. Amos, N. C. Handy, P. J. Knowles, J. E. Rice, and A. J. Stone, J. Phys. Chem. **89**, 2186 (1984).
[72] C. Adamo and V. Barone, J. Chem. Phys. **110**, 6158 (1999).
[73] A. J. Sadlej, Theor. Chim. Acta **81**, 339 (1992).
[74] M. Douglas and N. M. Kroll, Ann. Phys. (N.Y.) **82**, 89 (1974).
[75] J. Mitroy and J.-Y. Zhang, Phys. Rev. A **76**, 032706 (2007).
[76] R. Moszynski, P. S. Żuchowski, and B. Jeziorski, Collect. Czech. Chem. Commun. **70**, 1109 (2005).
[77] T. Korona, M. Przybytek, and B. Jeziorski, Mol. Phys. **104**, 2303 (2006).